Identification of Secondary Crashes on a Large-Scale Highway System

Dongxi Zheng, Madhav V. Chitturi, Andrea R. Bill, and David A. Noyce

Freeway incidents are major sources of nonrecurrent congestion, and resultant secondary crashes can prolong traffic impact and increase costs. Research on secondary crashes to support statewide transportation system management has been limited. In this study, a two-phase automated procedure was developed to identify secondary crashes on large-scale regional transportation systems. In the first phase, a crash-pairing algorithm was developed to extract spatially and temporally nearby crash pairs. The accuracy and efficiency of the algorithm were validated by comparing it to an ArcGIS-based program. In the second phase, two filters were proposed to reduce the crash pairs for secondary crash identification: the first filter selected crash pairs whose earlier crashes were on mainline highways; the second filter selected crash pairs whose later crashes happened within the dynamic impact areas (i.e., backup queues) of the earlier crashes. Shockwave theory was used to model the dynamic impact of a primary incident. The two-phase procedure used a linear referencing system for crash localization and can be applied to any regional transportation system with a similar data structure. A case study using 2010 data was conducted on nearly 1,500 mi of freeways in Wisconsin. Among the crash pairs produced by the two-phase procedure, 73 secondary crashes were confirmed with police reports. Preliminary analyses showed that (*a*) secondary crashes occurring in the same traffic direction as the primary incidents were about three times as frequent as secondary crashes in the opposing direction, and (*b*) two-vehicle rear-end collisions, multiple-vehicle rear-end collisions, and sideswipes were three major types of secondary crashes (about 84%).

The annual cost of congestion in the United States reportedly exceeds $120 billion (*1*). Freeway incidents are major sources of nonrecurrent congestion, and resulting secondary crashes can prolong traffic impact and increase costs. A secondary crash is an undesirable consequence of a primary incident. More formally, according to the FHWA, "secondary crashes are those that occur within the time of detection of the primary incident where a collision occurs either (*a*) within the incident scene or (*b*) within the queue, including the opposite direction, resulting from the original incident" (*2*). Existing studies have shown the extended traffic impact and the economic costs of secondary crashes (*3–5*). Reducing the chances of secondary crashes becomes a major consideration in the dispatch plans of traffic incident management agencies (*6, 7*).

D. Zheng, Room 1249A; M. V. Chitturi and A. R. Bill, Room B243; and D. A. Noyce, Room 1204, Traffic Operations and Safety Laboratory, Department of Civil and Environment Engineering, University of Wisconsin–Madison, Engineering Hall, 1415 Engineering Drive, Madison, WI 53706. Corresponding author: D. Zheng, dzheng3@wisc.edu.

Transportation Research Record: Journal of the Transportation Research Board, No. 2432, Transportation Research Board of the National Academies, Washington, D.C., 2014, pp. 82–90.
DOI: 10.3141/2432-10

Despite various findings on secondary crashes, most existing studies were limited by scope. Many were conducted on only one or two sample freeways or a short segment of highway; other studies extended the scope to freeways but considered a small regional scale. Only two studies were performed on a large scale that involved statewide highway systems. One major reason for such scope constraints was the challenge of identifying secondary crashes. To identify secondary crashes accurately, most existing studies considered the dynamic features of the traffic impact caused by the primary incidents. Thus, the study scopes were limited to highway facilities for which high-resolution traffic data were available for dynamic analyses. In addition, modeling the dynamic impact of primary incidents required considerable computational efforts, which for a statewide transportation system could be intolerable or even infeasible. Previous studies considering statewide highway systems did not consider the dynamic impact of primary incidents. In summary, none of the previous studies investigated secondary crashes on a statewide transportation system while considering the dynamic impact of primary incidents.

To fill the research gap identified above, the current study develops a two-phase automatic procedure. In the first phase, spatially and temporally nearby crash pairs (up to custom static thresholds) are extracted from a large network on the basis of a crash-pairing algorithm. The accuracy and the efficiency of this algorithm were validated. In the second phase, two filters are used to select crash pairs that are more likely to be primary–secondary crash pairs. One of the filters uses shockwave theory to evaluate the dynamic traffic impact of the primary incidents. At the end of the two-phase procedure, manual review of identified police reports is needed to confirm actual secondary crashes. However, the number of crash reports to review is considerably less.

LITERATURE REVIEW

Secondary crashes have been observed to be one of the notable consequences of freeway incidents. Early in the 1970s, Owens conducted an on-the-spot study of traffic incidents on a 21-km (13-mi) stretch of motorway in England during peak hours and found that 32.5% of the observed crashes were related to primary incidents (*8*). In recent decades, the development of intelligent transportation systems has made a variety of transportation data easier to access, which in turn has encouraged researchers to revisit secondary crashes. In earlier studies (*3–5, 9–17*), an incident was identified as a secondary crash as long as it occurred within a rectangular time–space window that originated from another incident. For example, Raub classified an incident as a secondary crash if it happened within 1,600 m upstream of another incident and no later than 15 min after that incident was cleared (*9, 10*). This type of method was called the "static threshold" in the sense that it considered the spatial impact range of a primary incident to be consistent throughout a certain period. However, the impact of a traffic incident is typically dynamic with respect to time.

Later studies incorporated this fact into secondary crash identification (*18–29*). The earliest attempt was made by Moore et al., who classified an incident as a secondary crash only if it fell under the progression curve (i.e., the resulting queue boundary as a function of time that is based on real-time data that tracks queue ends) of another incident (*5*). Curves with a similar concept were generated by using the traffic arrival–departure model in other studies (*20–22, 24*). In fact, these dynamic curves depicted only the moving queue fronts but did not consider the queue release from the incident location after the onset of incident clearance. To accommodate the releasing front, researchers have used either the speed contour map method or the ASDA [Automatische Staudynamikanalyse (automatic tracking of moving traffic jams)] model to depict the impact area of an incident (*19, 23, 25–29*). However, shockwave theory, which can also model the queuing and the releasing dynamics, has not been used in the literature for identifying secondary crashes.

Research on secondary crashes at the scale of a statewide transportation system has been limited. A majority of the existing studies focused on one or two sample freeways or only a stretch of a highway for which detailed traffic conditions could be obtained through densely deployed traffic detectors, closed-circuit traffic cameras, or even aircraft-based congestion-tracking systems (*4, 14, 16, 18, 19, 23, 25–28*). Some other studies extended the research scope to several freeways or urban arterials within a fully patrolled and intelligent transportation system–assisted district (*3, 5, 9, 10, 12, 13, 20–22, 24, 29*). Only a few studies were conducted on statewide transportation systems (*11, 17*). Identifying all spatially and temporally nearby crash pairs from a large highway network, and hence a significant number of input crashes, could be computationally complex. None of the above studies provided an efficient procedure.

On the basis of the preceding literature review, two primary objectives of the current study were set. First, an efficient algorithm to identify all nearby crash pairs (up to custom static thresholds) for a statewide transportation system should be developed. Second, to reduce the candidate primary–secondary crash pairs on the basis of static thresholds, additional filters that incorporate the dynamic feature of primary incident impact should be established.

DATA DESCRIPTION

The WisTransPortal data hub of the Traffic Operations and Safety laboratory at the University of Wisconsin–Madison houses a variety of statewide transportation data prepared and provided by the Wisconsin Department of Transportation (*30, 31*). Among these data, the state trunk network (STN) data and the crash data are the two primary inputs to the current study. The STN includes the state trunk highways, the U.S. highways (US), the Interstate highways (IHs), the designated freeways, and the expressways in Wisconsin as of 2012 (*32*). The crash data cover all reported crashes in Wisconsin since 1994 and are updated monthly. The Wisconsin Department of Transportation provides both the maps (i.e., Esri shapefiles) and the database records of the STN and crashes and also embeds a linear referencing system into the crash records to allow one to locate a crash on the STN without using the maps. For the proposed algorithm, the database records with the linear referencing system were used. The maps were used for validation and comparison purposes.

STN Links and Linear Referencing

A traditional way of modeling highway networks is to use a figure that consists of nodes and directional links. The STN is stored in this manner. Nodes in the STN are called reference sites (RSs). Each link in the STN starts from one RS (RS^{from}) and ends at another RS (RS^{to}). A link represents a highway segment, either mainline or ramp, in one traffic direction with relatively consistent geometric layout (e.g., number of lanes, lane width, etc.). Figure 1 illustrates

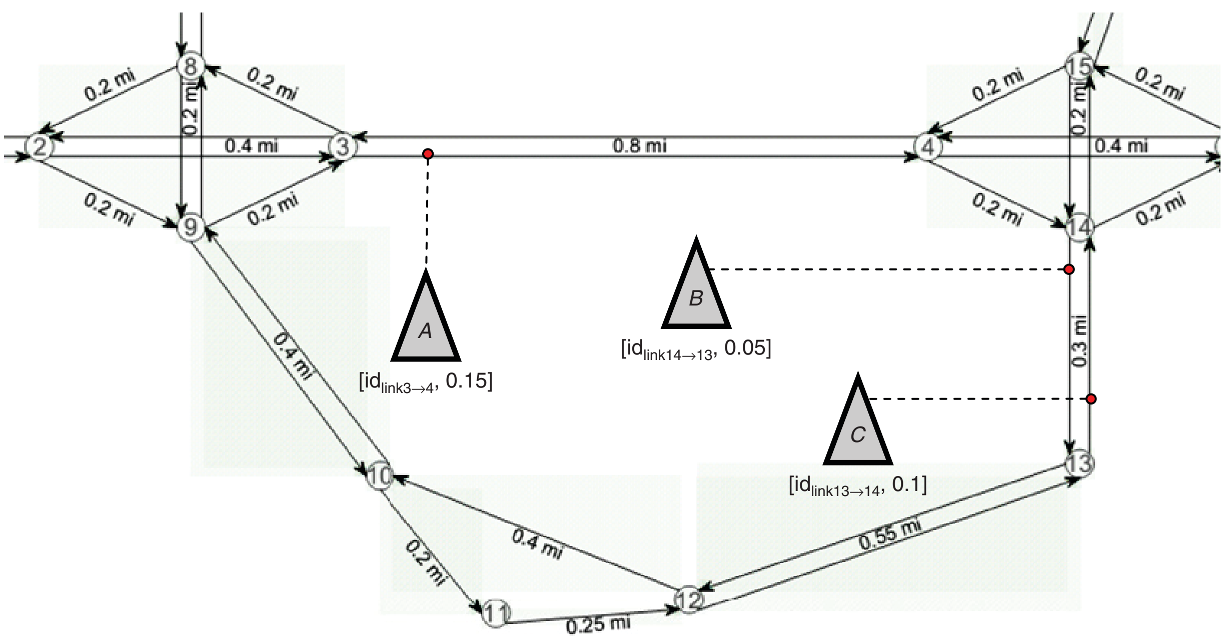

Example distances:

$d(A,B) = (0.8 - 0.15) + 0.2 + (0.3 - 0.05) = 1.1$ mi

$d(B,C) = 0.3 - 0.05 - 0.1 = 0.15$ mi

FIGURE 1 Example of linear referencing system.

the representation of a small portion of a highway network in the STN. Links are displayed as solid arrows with their lengths. RSs are labeled in circles. An arbitrary location on the STN, for example, a crash scene, is determined by a linear coordinate (link id, link offset), namely linear referencing. The link id identifies the link in which the crash occurred, and the link offset tells the distance from the link's RS^{from} to the crash. As of 2012, the number of in-operation links was 33,015 and the total length 24,903 mi.

Crash Records

WisTransPortal stores each reported crash in Wisconsin as a record in the database. Each crash record contains detailed information about the crash, such as a unique identification number, date, time, link id, and link offset of the crash location (for linear referencing). In addition, each crash record is associated with a document id that links the crash to its police report, Form MV4000, which provides additional information such as that on any police investigation and a crash diagram.

Other Data

In addition to the STN links, WisTransPortal also stores other highway information. For example, all the routes in STN are stored in a table, each record representing the entire stretch of a highway route and its geographical direction (e.g., US-12 eastbound); virtual mile markers are stored as reference points. Traffic data are also available. The Wisconsin Department of Transportation manages the TRaffic DAta System (TRADAS) and the Advanced Transportation Management System, with traffic detectors deployed on the STN. WisTransPortal contains information of these TRADAS and Advanced Transportation Management System detectors as well as their traffic counts.

FIRST PHASE: CRASH-PAIRING ALGORITHM

Given the STN linear-referencing system and the crash records, the target of the crash-pairing algorithm is to identify all crash pairs (c_i, c_j) that satisfy Formulas 1 and 2. In Formula 2, $d(c_i, c_j)$ is measured along the STN links by treating the links as bidirectional (see examples in Figure 1). Highway splits, merges, and intersections should be accommodated, a need that was not addressed by previous studies focusing on individual freeways.

$$0 \le t(c_j) - t(c_i) \le T \tag{1}$$

$$d(c_i, c_j) \le D \tag{2}$$

where

c_i = crash i (former crash),
c_j = crash j (later crash),
$t(c)$ = time of crash c since an early time origin (min),
$d(c_i, c_j)$ = network distance between crash c_i and c_j (mi),
T = time window (threshold, min), and
D = space window (threshold, mi).

Given the significant sizes of the STN links and the crashes, simple algorithms are either slow or infeasible. One naive algorithm runs Dijkstra's method repeatedly for every crash. Dijkstra's method is an iterative approach that finds the shortest path from an origin (O) to every node in a network. A brief summary of Dijkstra's method follows. All nodes are considered to be infinitely distant from the origin and are "unvisited" initially. The method begins from the origin and computes the distances to its neighbors (i.e., nodes with direct connection) and marks the origin as "visited." In every successive iteration step, the method chooses the closest unvisited node to the origin, updates the distances from the origin to that node's unvisited neighbors if the paths become shorter through that node, and marks that node as visited. The iteration continues until every node is visited. At the end, the distances from the origin to each node are the shortest distances (*33*). The complexity of Dijkstra's method is $O(N^2)$ with respect to N crashes, where N is larger than 100,000 for an annual statewide analysis. By repeatedly using Dijkstra's method for N crashes, the complexity of the naive algorithm becomes $O(N^3)$, which is not efficient. Another alternative is to use dynamic programming to populate a shortest-path matrix between every two crashes. This alternative is infeasible because it not only spends an equivalent amount of computation time as the first algorithm but also requires unacceptable computer memory space (e.g., $100{,}000^2 * 8$ bytes $\approx$ 75 GB) to store the matrix.

The proposed pairing algorithm first analyzes the relationships between links and uses these relationships to derive crash-to-crash distances. For each link lk_i that contains one or more crashes, the algorithm performs a variant of Dijkstra's traversal (as will be explained later) and generates the relationships between lk_i and the other links. The distances between crashes are then calculated on the basis of these relationships. Compared with the first algorithm mentioned above, here the number of traversals is bounded by the total number of links no matter how many crashes are analyzed. The pairing algorithm also uses the space window of D miles to constrain Dijkstra's traversal to a relevant portion (normally small) of the STN network. In the following subsections, the concept of a local linear-coordinate system is introduced; the system is based on the relationship between two links that can be comprehensively defined. Furthermore, the equation for deriving crash-to-crash distance from the link-to-link relationship is also given, along with the concept of a candidate link that is used to constrain Dijkstra's traversals, the pseudo-code of the algorithm with a special case explanation, and finally, the validation of this algorithm.

Local Linear-Coordinate System

A local linear-coordinate system (LLCS) is defined for each link, namely a base link, to describe the spatial relationship between any RS and the base link. Let RS^{from}_{base} and RS^{to}_{base} denote the from reference site and the to reference site of the base link. Under the LLCS, each RS in the network has a two-fold coordinate with the following definitions:

- Forward (positive) coordinate (x^+_{RS}) = the length of the base link + $d(RS^{to}_{base}, RS) \mid RS^{from}_{base}$. The $d(RS^{to}_{base}, RS) \mid RS^{from}_{base}$ is the shortest network distance between RS^{to}_{base} and RS in a subnetwork without RS^{from}_{base} (and links connected to it). If $d(RS^{to}_{base}, RS) \mid RS^{from}_{base}$ does not exist, $x^+_{RS} = +\infty$. Specifically, $x^+_{RS^{from}_{base}}$ is defined as 0.
- Backward (negative) coordinate (x^-_{RS}) = $d(RS^{from}_{base}, RS) \mid RS^{to}_{base}$. The $d(RS^{from}_{base}, RS) \mid RS^{to}_{base}$ is the shortest network distance between RS^{from}_{base} and RS in a subnetwork without RS^{to}_{base} (and links connected to it). If $d(RS^{from}_{base}, RS) \mid RS^{to}_{base}$ does not exist, $x^-_{RS} = +\infty$. For example, $x^-_{RS^{to}_{base}} = +\infty$.

As an example, in Figure 1, consider RS_{12} under the LLCS of $link_{3\to4}$ (as the base link). The $x^+_{RS_{12}} = 0.8$ ($link_{3\to4}$) + 0.2 ($link_{4\to14}$) +

0.3 ($\text{link}_{14\to13}$) + 0.55 ($\text{link}_{13\to12}$) = 1.85 mi. The $x^-_{\text{RS}_{12}}$ = 0.2 ($\text{link}_{9\to3}$) + 0.4 ($\text{link}_{10\to9}$) + 0.4 ($\text{link}_{12\to10}$) = 1.0 mi.

A variant of Dijkstra's shortest path traversal can be used to calculate the LLCS coordinates of all RSs on the fly. The traversal is divided into two passes. In the first pass, Dijkstra's algorithm starts from $\text{RS}^{\text{to}}_{\text{base}}$ and expands to the rest of the network while ignoring all links connected to $\text{RS}^{\text{from}}_{\text{base}}$. During the traversal, the forward coordinates of all reached RSs are calculated or updated. Similarly, in the second pass, Dijkstra's algorithm starts from $\text{RS}^{\text{from}}_{\text{base}}$ and ignores all links connecting to $\text{RS}^{\text{to}}_{\text{base}}$, filling the backward coordinates of all reached RSs.

In the context of an LLCS, any link (including the base link) is related to the base link by the LLCS coordinates of its RS^{from} and RS^{to}. Specifically, let a link to be related to the base link be called a test link and its end RSs be denoted as $\text{RS}^{\text{from}}_{\text{test}}$ and $\text{RS}^{\text{to}}_{\text{test}}$. Vector $v_{\text{test}} = [x^+_{\text{RS}^{\text{from}}_{\text{test}}}, x^-_{\text{RS}^{\text{from}}_{\text{test}}}, x^+_{\text{RS}^{\text{to}}_{\text{test}}}, x^-_{\text{RS}^{\text{to}}_{\text{test}}}]$ is defined as the relationship vector of the test link in the LLCS. With the relationship vector, the network distance between a crash c_{base} on the base link and a crash c_{test} on a test link can be easily calculated by using Equations 3 through 7. Because the four coordinates in the relationship vector might result from different routings, four crash-to-crash distances are possible (Equations 4 through 7), and their geometric meanings are demonstrated in Figure 2. The final crash-to-crash distance should be the smallest possible distance. Besides determining the distance value, one can also tell whether the two crashes were in the same traffic direction. For example, if the final distance is d^+_F (Figure 2*a*), the centerline of the resulting route becomes bolded and the traffic directions of both crashes (green arrows) are on the same side of the centerline, meaning that the two crashes (or links) were in the same traffic direction; otherwise, like d^+_T and d^-_F and (Figure 2, *b* and *c*), the two crashes were in opposite traffic directions. In addition, one can also determine whether c_{test} happened upstream or downstream of c_{base}. For instance, c_{test} happened upstream of c_{base} if d^+_T (Figure 2*b*) or d^-_T (Figure 2*d*) is the final distance (when the test crash direction follows the bolded route); otherwise, c_{test} happened downstream of c_{base} (when the test crash direction departs from the bolded route).

$$d\left(c_{\text{base}}, c_{\text{test}}\right) = \min\left(d^+_F, d^+_T, d^-_F, d^-_T\right) \tag{3}$$

$$d^+_F = x^+_{\text{RS}^{\text{from}}_{\text{test}}} - \text{os}_{\text{base}} + \text{os}_{\text{test}} \tag{4}$$

$$d^+_T = x^+_{\text{RS}^{\text{to}}_{\text{test}}} - \text{os}_{\text{base}} + \left(l_{\text{test}} - \text{os}_{\text{test}}\right) \tag{5}$$

$$d^-_F = x^-_{\text{RS}^{\text{from}}_{\text{test}}} + \text{os}_{\text{base}} + \text{os}_{\text{test}} \tag{6}$$

$$d^-_T = x^-_{\text{RS}^{\text{to}}_{\text{test}}} + \text{os}_{\text{base}} + \left(l_{\text{test}} - \text{os}_{\text{test}}\right) \tag{7}$$

where

$d(c_{\text{base}}, c_{\text{test}})$ = network distance between c_{base} and c_{test} (mi),
d^+_F = possible distance by way of $\text{RS}^{\text{from}}_{\text{test}}$ forward coordinate (mi),
d^+_T = possible distance by way of $\text{RS}^{\text{to}}_{\text{test}}$ forward coordinate (mi),
d^-_F = possible distance by way of $\text{RS}^{\text{from}}_{\text{test}}$ backward coordinate (mi),
d^-_T = possible distance by way of $\text{RS}^{\text{to}}_{\text{test}}$ backward coordinate (mi),

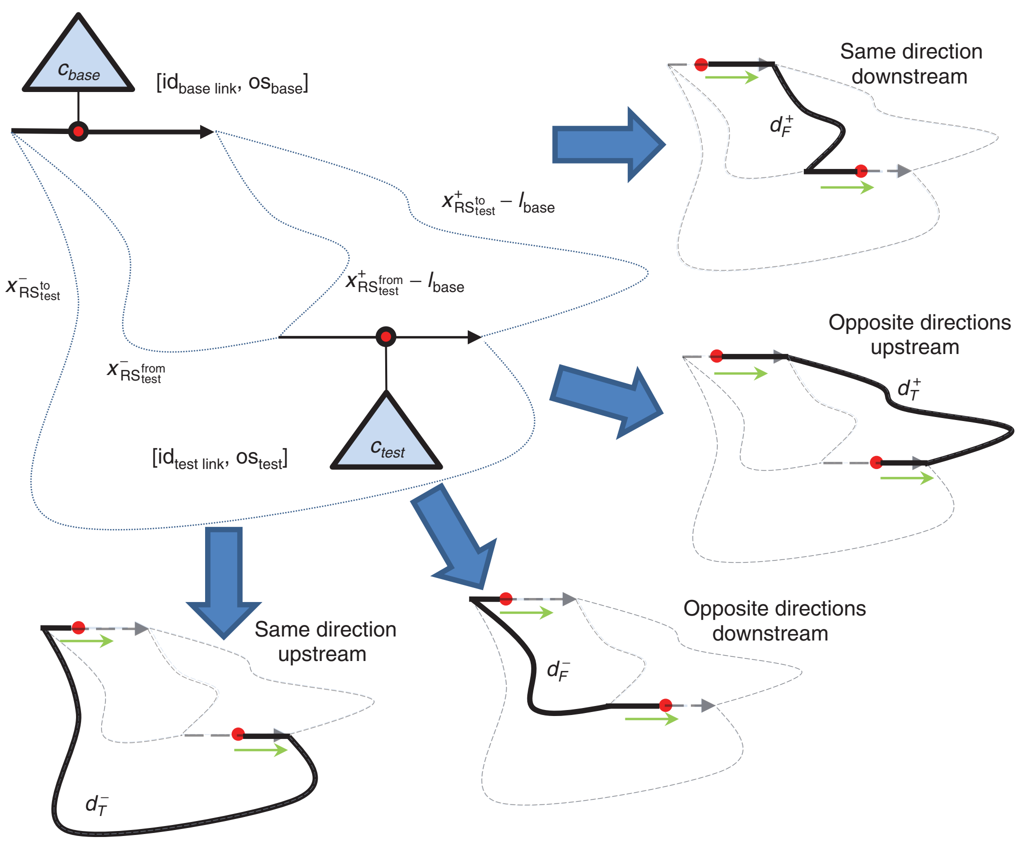

FIGURE 2 Four possible distances between two crashes on basis of relationship vector.

$x^{+}_{\mathrm{RS}^{\mathrm{from}}_{\mathrm{test}}}$ = forward coordinate of $\mathrm{RS}^{\mathrm{from}}_{\mathrm{test}}$ (mi),
$x^{-}_{\mathrm{RS}^{\mathrm{from}}_{\mathrm{test}}}$ = backward coordinate of $\mathrm{RS}^{\mathrm{from}}_{\mathrm{test}}$ (mi),
$x^{+}_{\mathrm{RS}^{\mathrm{to}}_{\mathrm{test}}}$ = forward coordinate of $\mathrm{RS}^{\mathrm{to}}_{\mathrm{test}}$ (mi),
$x^{-}_{\mathrm{RS}^{\mathrm{to}}_{\mathrm{test}}}$ = backward coordinate of $\mathrm{RS}^{\mathrm{to}}_{\mathrm{test}}$ (mi),
$\mathrm{os}_{\mathrm{base}}$ = link offset of c_{base} (mi),
$\mathrm{os}_{\mathrm{test}}$ = link offset of c_{test} (mi), and
l_{test} = length of test link (mi).

Candidate Link

In the previous section, every link is assumed to be tested against the base link. However, given a particular spatial threshold of D miles, a test link too far from the base link is irrelevant to finding the nearby crash pairs. Only those links whose relationship vectors satisfy a certain condition may contain crashes within D miles of the base link crashes. In fact, the condition is as simple as $\min (x^{+}_{\mathrm{RS}^{\mathrm{from}}_{\mathrm{test}}} - l_{\mathrm{base}}, x^{-}_{\mathrm{RS}^{\mathrm{from}}_{\mathrm{test}}}, x^{+}_{\mathrm{RS}^{\mathrm{to}}_{\mathrm{test}}} - l_{\mathrm{base}}, x^{-}_{\mathrm{RS}^{\mathrm{to}}_{\mathrm{test}}}) \leq D$, where l_{base} is the length of the base link. Links satisfying this condition are called candidate links and form a relatively small and relevant portion of the network (when D is relatively small). The two passes of Dijkstra's traversal can stop expansion as early as any further RS to be reached has a forward coordinate larger than $l_{\mathrm{base}} + D$ and a backward coordinate larger than D. Then, all links connected to the already-reached RSs are all the candidate links.

Algorithm

The pseudo-code of the proposed crash pairing algorithm is shown below. Here L_{base} is assumed to be a preprocessed set of links containing at least one crash. The statement "find all candidate links" refers to the preparation of the relationship vectors for all candidate links in the LLCS as described earlier. The function $t(*)$ is the function for getting the time of a crash in minutes since a consistent time origin. T and D are the static thresholds in minutes and miles, respectively. The recorded time of a crash could be slightly different from the time when the crash occurred. However, the authors do not expect it to have a significant impact on the results because a large time threshold of 5 h was used. The statement "calculate $d(c_{\mathrm{base}}, c_{\mathrm{cand}})$" (where "cand" means candidate), refers to Equations 3 through 7.

For each $\mathbf{lk_{base}}$ in $\boldsymbol{L}_{\mathbf{base}}$:
Find all candidate links of $\mathbf{lk_{base}}$ as a set $\boldsymbol{L}_{\mathbf{cand}}$;
For each candidate link $\mathbf{lk_{cand}}$ in $\boldsymbol{L}_{\mathbf{cand}}$,
For each crash $\boldsymbol{c}_{\mathbf{base}}$ in $\mathbf{lk_{base}}$,
For each crash $\boldsymbol{c}_{\mathbf{cand}}$ in $\mathbf{lk_{cand}}$, and
If $0 \leq t(\boldsymbol{c}_{\mathbf{cand}}) - t(\boldsymbol{c}_{\mathbf{base}}) \leq \boldsymbol{T}$:
Calculate $d(\boldsymbol{c}_{\mathbf{base}}, \boldsymbol{c}_{\mathbf{cand}})$;
If $d(\boldsymbol{c}_{\mathbf{base}}, \boldsymbol{c}_{\mathbf{cand}}) \leq \boldsymbol{D}$:
Add $(\boldsymbol{c}_{\mathbf{base}}, \boldsymbol{c}_{\mathbf{cand}})$ as a pair in the result.

A special case should be treated differently. As Figure 1 shows, the longitudinal distance between Crashes B and C was only 0.15 mi, but they occurred on opposite sides of the same highway. However, if one relies only on the network traversal of links, the resulting distance will go around RS_{14} (upper right in Figure 1) and be calculated as 0.25 mi. Such an unrealistic result is not desirable. To overcome this limitation, additional information from the STN was employed. An STN table of route links was used to aid the links with their physical meanings. Each record in the route link table specifies the both the highway to which a link belongs and the direction. All links on the other side of the same highway are considered candidate links of the base link. When the distance is being calculated between a crash on the base link and a crash on the other side of the highway, the algorithm calculates the cumulative distances from the two crashes to a far upstream–downstream shared RS on the highway. The difference between these two cumulative distances is considered the distance between these two crashes. Furthermore, when a shared RS cannot be found, the algorithm further uses another set of highway reference locations, reference points (RPs). Each RP has its on-highway number, on-highway direction, RP number, and RP letter. If two RPs have the same on-highway number, RP number, and RP letter, they correspond to the same longitudinal position on the highway, even with different on-highway directions. In addition, each RP, like a crash location, has a linear reference that maps it onto a link. On the basis of the preceding input, if two links on opposite sides of the same highway contains RPs with the same RP number and RP letter, they share a longitudinal position. Thus, instead of looking for a shared RS, the algorithm looks for a shared longitudinal position that is based on RPs.

Validation

The pairing algorithm was implemented as a Java program. The program passed several small independent tests (e.g., the entire stretch of a particular highway in the STN with crashes of several days) with manually extracted ground truths. To validate the accuracy and the efficiency of the algorithm further, a large-scale network was tested. Because manual extraction of the ground truth in the large-scale test was infeasible, a relatively reliable ArcGIS-based program was used as a mutual validation reference. The basic idea of the ArcGIS-based program is to prepare a network data set by using the STN shapefile and the crash shapefile and to employ the buffer function of the NetworkAnalyst toolbox to find, for each crash, every other crash that is within a buffer network distance (spatial threshold) from that crash. The ArcGIS-based program was implemented in C++ by using ArcGIS APIs. Because of the unavailability of control over the buffer function of the NetworkAnalyst toolbox, the ArcGIS-based program was similar to the naive algorithm of traversing the network for every pair of crashes, which provided the authors a chance to compare efficiencies.

Both the pairing algorithm and the ArcGIS-based program were tested on 10,922 crashes from a freeway network of about 1,500 total miles in Wisconsin in 2010, with $D = 10$ mi and $T = 5$ h. The pairing algorithm yielded 15,901 crash pairs while the ArcGIS-based program yielded 13,850 crash pairs. Both systems captured the same 13,594 crash pairs. The ArcGIS-based program captured 256 extra pairs, which were later found to be missed by the pairing algorithm because of computer precision problems but did not hurt the validity of the pairing algorithm. The pairing algorithm captured 2,307 extra pairs that were correct output but missed by the ArcGIS-based program. In summary, the pairing program correctly identified more crash pairs than the ArcGIS-based program. In addition, the ArcGIS-based program finished the analysis in 2½ days, while the pairing algorithm finished in about 2 h (30 times as fast).

SECOND PHASE: CRASH PAIR FILTERS

For the purpose of identifying secondary crashes, the pairing algorithm produces an initial searching set, which, without additional filtering, could be too vast to be useful. Proposed below are two filters for selecting crash pairs that are more likely to capture a primary–secondary relationship.

Ramp Filter

A crash pair resulting from the proposed algorithm will be excluded if its former crash happened on a highway on- or off-ramp. A crash is determined to be on a ramp if the link on which it happened represents a portion or an entire segment of a ramp. The rationale behind this filter is that ramp crashes rarely cause secondary crashes. To evaluate this assumption, 85 sample crash pairs whose former crashes happened on a ramp were selected and verified. One or two crash pairs were randomly sampled from each 1-h, 5-mi interval of the 5-h, 10-mi thresholds. Manual review showed that none of the 85 samples contained a primary–secondary pair. Although one crash pair involved two secondary crashes, they were not related; in addition, these two secondary crashes were captured by the actual primary–second pairs whose primary crashes were not on ramps.

Impact Area Filter

As noted in the literature review, crash pairs resulting from static thresholds could contain false primary–secondary pairs. These false pairs generally have unreasonable combinations of time and spatial distances. For example, a candidate pair with time distance of 0 min and spatial distance of 5 mi is certainly not a primary–secondary crash pair. Because secondary crashes have been recognized as in the queue caused by the primary incidents, queue theories were commonly used to establish the time-varying impact area of the primary incidents to identify secondary crashes (*13, 14, 18–29*). Comparison of various queue estimation methods can be found in more-general traffic research papers (*34, 35*). The literature review indicates that none of the previous secondary crash studies used the shockwave model to estimate the impact area caused by a primary incident. In the current study, the impact area of a crash is defined between two simplified straight shockwave lines, one for the queuing shockwave and the other for the discharging shockwave (Figure 3). Mathematical representation for judging whether a crash fell into the impact area of another is given in Equations 8 through 10. Traffic flow of the prevailing traffic condition (q_1) is the monthly average hourly traffic volume provided by the TRADAS detectors, with the same day of week and the same hour of the day as the former crash. If the later crash occurred outside the impact area and its parallel portion on the opposite traffic direction of the former crash, the crash pair would be excluded. However, secondary crashes could occur in the vicinity of the primary incident during its clearance. This type of secondary crash was typically attributed to the rubbernecking effect (*8, 36*). To capture these secondary crashes, a crash pair whose spatial distance (upstream or downstream in either traffic direction) was no larger than 1 mi and whose temporal distance was no larger than 1 h should be preserved, even if it does not satisfy the impact area requirement.

$$a_2 \times (t - t_{\text{clearance}}) \le d \le a_1 \times t \tag{8}$$

$$a_1 = \frac{(q_2 - q_1)}{(k_2 - k_1)} \tag{9}$$

$$a_2 = \frac{(q_3 - q_2)}{(k_3 - k_2)} \tag{10}$$

where

t = time between former crash and later crash (h);
$t_{\text{clearance}}$ = 1 h (simplified crash clearance time);
d = network distance between the two crashes (mi);
a_1 = queuing shockwave speed (mph);
a_2 = release shockwave speed (mph);
q_1 = traffic flow of prevailing condition [vehicles per hour per lane (vphpl)];
k_1 = density of prevailing condition (vphpl), with 65 mph assumed as the prevailing speed as a simplification and $k_1 = q_1/65$;
q_2 = 0 vphpl (traffic flow of jam condition);
k_2 = 352 vehicles per mile per lane (vpmpl) (density of jam condition, which assumes minimum of 15 ft head-to-head distance between vehicles);
q_3 = 1,900 vphpl (traffic flow of saturated condition); and
k_3 = 1,900/65 vpmpl (density of saturated condition).

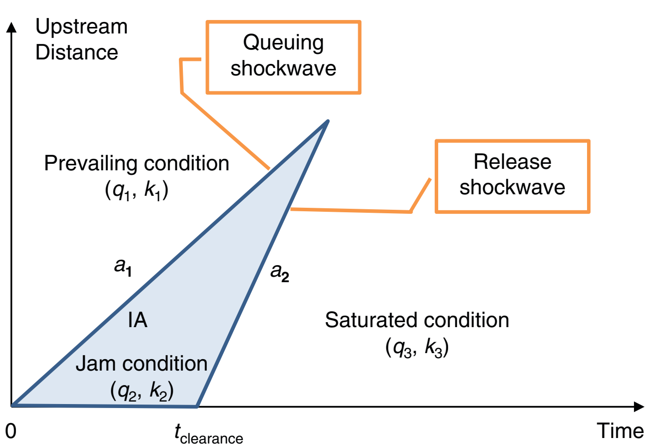

FIGURE 3 Example of impact area (IA).

CASE STUDY

A case study was conducted on crashes that occurred on approximately 1,500 mi of freeways in Wisconsin during 2010. The layout of these freeways in relation to the entire STN network is shown in the map in Figure 4. Although the case study used only crashes occurring on these freeways, the calculation of network distances was not subjected to these freeways but instead relied on the entire STN network. A total of 12,513 raw input crashes were retrieved for 2010, the last 5 h of 2009, and the first 5 h of 2011. The inclusion of 5 h into both the previous and the next year corresponds to the selected 5-h temporal threshold so that crash pairs crossing the new year's boundary could be captured. The workflow and the resultant reduced data in each step are summarized in the flow diagram in Figure 4.

(In Figure 4, the number of distinct crashes in parentheses is normally smaller than twice the corresponding number of crash pairs because one crash might be captured in more than one crash pair. The total number of crash pairs before and after a branching point remains the same. However, because a crash might be involved in two crash pairs belonging to different branches, the sum of the numbers of distinct crashes is normally larger than the number of crashes before the branching point.)

Before the pairing algorithm was applied, the raw input crashes were first reduced on the basis of a focused study scope that excluded inclement weather conditions and deer crashes. In Wisconsin, a large

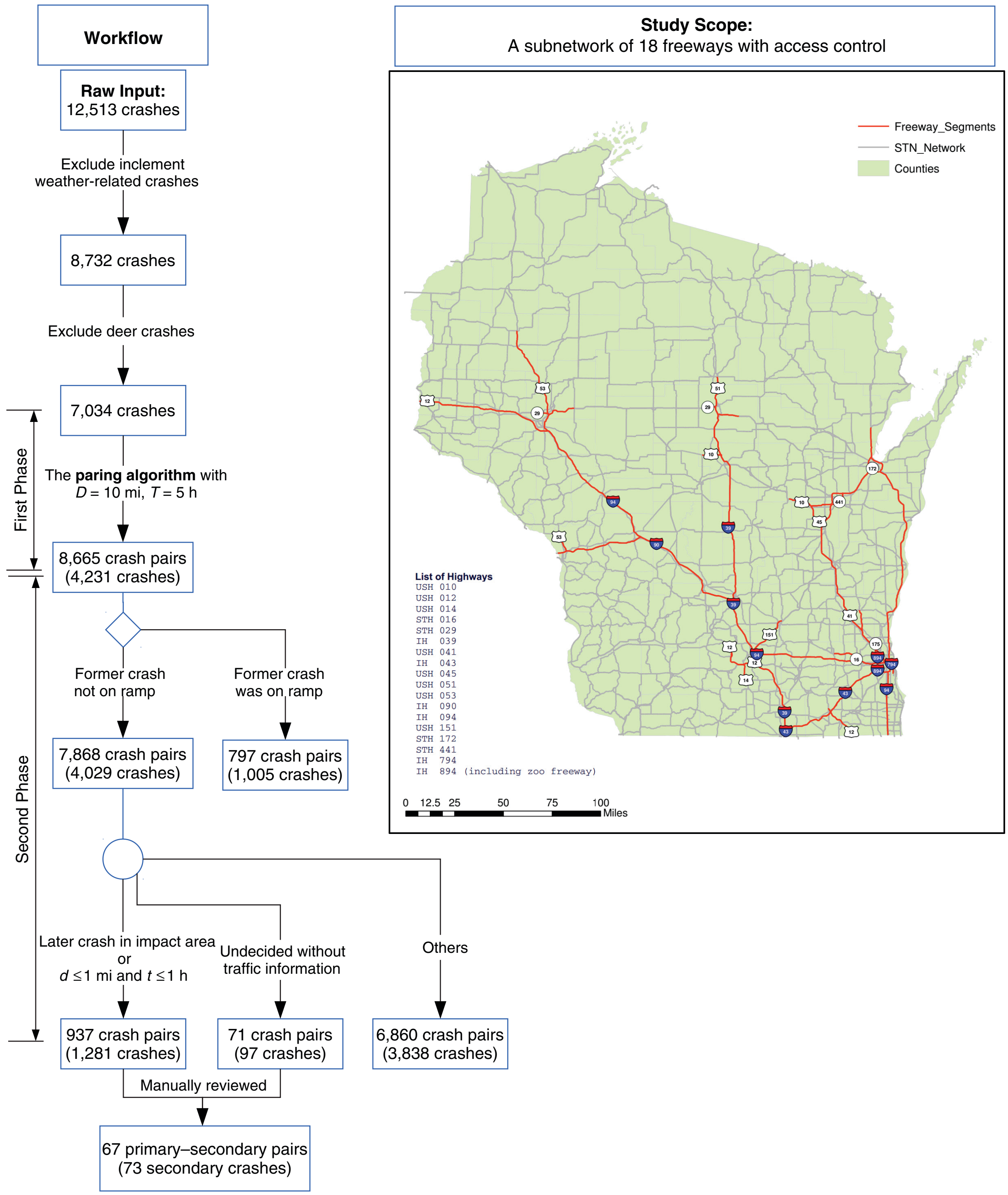

FIGURE 4 Summary of case study for 2010 [raw input = all crashes happened on 18 freeways (mainline and ramps) in 2010, last 5 h of 2009, and first 5 h of 2011; in impact area = both upstream of former crash location in its traffic direction and downstream in opposite traffic direction].

portion of crashes are related to inclement weather during the winter. For example, in January 2010, 1,520 of 3,592 crashes (about 42%) on Wisconsin state trunk highways occurred during or after snow or rain. Some circumstances, such as successive run-off-the-road crashes in snowstorms and back-to-back rear-end crashes attributable to slippery or icy roads were recognized as contributing to secondary crashes. However, weather is out of the control of traffic incident management agencies. Because the current research is focused on secondary crashes that are more likely to be prevented by effective traffic incident management, inclement weather–related crashes were not included in this study, but the authors intend to study them separately in the future. For a similar reason, deer crashes (about 20% of the total) were excluded from the study. As a result, 7,034 crashes remained as the input to the proposed algorithm.

Conservative thresholds of 10 mi and 5 h were used for the first phase (crash pairing). The 10-mi, 5-h thresholds are approximately 5 times as large (in each dimension) as most static thresholds used in the literature and supersede all actual temporal–spatial ranges of primary–second pairs found by existing studies (*3–5, 9–14, 16–29*). Thus, the use of even larger thresholds is unlikely to include more actual primary–secondary crash pairs. The pairing algorithm generated 8,665 crash pairs (4,231 distinct crashes). The second phase (crash pair filtering) further reduced the number of crash pairs to 1,008 (88.4% reduction). To this point in the analysis, all computations were completed automatically within 2 h. The resultant 1,008 crash pairs for manual review contained only 1,342 distinct crashes. Compared with the initial input of 7,034 crashes, the crash-pairing and filtering procedures reduced the number of crashes needing review by 81%.

Secondary crashes and their corresponding primary incidents were confirmed through manual review of police reports. Approximately 30 person-hours were used in reviewing the 1,008 candidate crash pairs; this number averaged to nearly two person-minutes per crash pair. Potential employment of optical character recognition and artificial intelligence may help in further minimizing the reviewing time in the future. A crash was classified as a secondary crash only when its report explicitly referred to a previous crash. This criterion might have resulted in fewer secondary crashes than occurred but ensured the confidence of further analyses on the resulting secondary crashes. Primary incidents were identified only if they could be matched, by either document number or other key descriptions, to those referred by the secondary crashes. By these criteria, 73 crash pairs were found to contain secondary crashes. The number of distinct secondary crashes was also 73. Among the 73 pairs, 67 captured the primary incidents.

Preliminary analyses were conducted on the resulting primary–secondary pairs and secondary crashes. Among the 67 primary–secondary pairs, 52 secondary crashes (77.6%) occurred in the same traffic direction as the primary crashes, and the average spatial and temporal distances were 1,520 ft and 15.2 min, respectively; 15 secondary crashes (22.4%) occurred in the opposite traffic direction of the primary crashes, and the average spatial and temporal distances were 1,197 ft and 17.4 min, respectively. Among the 73 secondary crashes, 40 were two-vehicle rear-ends collisions (54.8%), 10 multiple-vehicle rear-end collisions (13.7%), 11 sideswipes (15.1%), five hitting debris (6.8%), two angle crashes (2.7%), three with squad vehicles on primary crash scenes (4.1%), and one losing control (1.4%).

CONCLUSIONS, RECOMMENDATIONS, AND FUTURE WORK

Secondary crashes are known to prolong the nonrecurrent congestion caused by primary freeway incidents. The benefit of reducing secondary crashes has also been found to exceed traffic incident management countermeasures, such as freeway patrol services. However, research on secondary crashes on large regional transportation systems was limited. The current study contributes to the research community with the following efforts and findings:

- An efficient crash-pairing algorithm was developed to extract spatially and temporally nearby (up to custom static thresholds) crash pairs from a large-scale regional transportation system. The accuracy and efficiency of this algorithm were validated.
- Two effective filters were proposed to select crash pairs that were more likely to capture primary–secondary relationships. The first filter restricts the primary incidents on mainline highways. The second filter restricts the secondary crashes to be within the dynamic impact areas of the primary incidents. Shockwave theory is first used by the current study to estimate the dynamic impact area of a primary incident.
- A two-phase procedure consisting of the pairing algorithm and filters automatically narrows the searching space for secondary crashes in a large regional transportation system. Although the procedure is based on the commonly used linear referencing system for crash localization, any transportation system with similar data representation can be analyzed with the procedure. A manual review of the effectively narrowed search space is required.
- A case study for crashes occurring in 2010 on about 1,500 mi of Wisconsin freeways was conducted. From the crash pairs extracted by using the two-phase procedure, 73 secondary crashes were confirmed via careful manual review of police reports. Secondary crashes occurring in the same traffic direction of the primary incidents were about three times those occurring in the opposite direction. Two-vehicle rear-end collisions, multiple-vehicle rear-end collisions, and sideswipes were three major types of secondary crashes (about 84%). Other crash types, such as hitting debris, angle crashes, losing control, and striking squad vehicles were also observed.

Three major efforts for future work are recommended. First, to make the whole workflow of secondary crash identification more automatic, optical character recognition and artificial intelligence might be employed to assist human reviewers in examining police reports. Second, more years of data must be collected to establish a larger sample of secondary crashes for more comprehensive statistical analyses. Finally, because the objective of this study was to analyze secondary crashes that can be mitigated by traffic incident management strategies, crashes in inclement weather were not included. The authors realize that secondary crashes occur in inclement weather and recommend that future studies examine the impact of weather on secondary crashes.

ACKNOWLEDGMENTS

The authors gratefully acknowledge support of this study by Paul Keltner of the Bureau of Traffic Operations, Wisconsin Department of Transportation. Special thanks go to the staff of the Traffic Operations and Safety laboratory, especially Steven Parker, who manages the WisTransPortal and provided technical support.

REFERENCES

1. Schrank, D., B. Eisele, and T. Lomax. *TTI's 2012 Urban Mobility Report.* Texas Transportation Institute, Texas A&M University System, College Station, Texas, 2012.
2. Margiotta, R., R. Dowling, and J. Paracha. *Analysis, Modeling, and Simulation for Traffic Incident Management Applications.* FHWA-HOP-12-045. FHWA, U.S. Department of Transportation, 2012.
3. Khattak, A. J., X. Wang, and H. Zhang. Are Incident Durations and Secondary Incidents Interdependent? In *Transportation Research Record: Journal of the Transportation Research Board, No. 2099,* Transportation Research Board of the National Academies, Washington, D.C., 2009, pp. 39–49.
4. Karlaftis, M. G., S. P. Latoski, N. J. Richards, and K. C. Sinha. ITS Impacts on Safety and Traffic Management: An Investigation of Secondary Crash Causes. *Journal of Intelligent Transportation Systems,* Vol. 5, No. 1, 1999, pp. 39–52.

5. Moore, J.E., II, G. Giuliano, and S. Cho. Secondary Accident Rates on Los Angeles Freeways. *Journal of Transportation Engineering,* Vol. 130, No. 3, 2004, pp. 280–285.
6. Owens, N., A. Armstrong, P. Sullivan, C. Mitchell, D. Newton, R. Brewster, and T. Trego. *Traffic Incident Management Handbook.* FHWA-HOP-10-013. FHWA, U.S. Department of Transportation, 2010.
7. Dunn, W.M., and S.P. Latoski. *NCHRP Synthesis of Highway Practice 318: Safe and Quick Clearance of Traffic Incidents.* Transportation Research Board of National Academies, Washington, D.C., 2003.
8. Owens, O. *Traffic Incidents on the M1 Motorway in Hertfordshire.* Transport and Road Research Laboratory, Crowthorne, United Kingdom, 1978.
9. Raub, R.A. Secondary Crashes: An Important Component of Roadway Incident Management. *Transportation Quarterly,* Vol. 51, No. 3, 1997, pp. 93–104.
10. Raub, R. Occurrence of Secondary Crashes on Urban Arterial Roadways. In *Transportation Research Record 1581,* TRB, National Research Council, Washington, D.C., 1997, pp. 53–58.
11. Hirunyanitiwattana, W., and S.P. Mattingly. Identifying Secondary Crash Characteristics for California Highway System. Presented at 85th Annual Meeting of the Transportation Research Board, Washington, D.C., 2006.
12. Zhan, C., L. Shen, M.A. Hadi, and A. Gan. Understanding the Characteristics of Secondary Crashes on Freeways. Presented at 87th Annual Meeting of the Transportation Research Board, Washington, D.C., 2008.
13. Zhan, C., A. Gan, and M.A. Hadi. Identifying Secondary Crashes and Their Contributing Factors. In *Transportation Research Record: Journal of the Transportation Research Board, No. 2102,* Transportation Research Board of the National Academies, Washington, D.C., 2009, pp. 68–75.
14. Vlahogianni, E.I., M.G. Karlaftis, J.C. Golias, and B.M. Halkias. Freeway Operations, Spatiotemporal-Incident Characteristics, and Secondary-Crash Occurrence. In *Transportation Research Record: Journal of the Transportation Research Board, No. 2178,* Transportation Research Board of the National Academies, Washington, D.C., 2010, pp. 1–9.
15. Khattak, A.J., X. Wang, H. Zhang, and M. Cetin. *Primary and Secondary Incident Management: Predicting Durations in Real Time.* Report VTRC 87648. Virginia Transportation Research Council, Charlottesville, 2009.
16. Kopitch, L., and J.-D.M. Saphores. Assessing Effectiveness of Changeable Message Signs on Secondary Crashes. Presented at 90th Annual Meeting of the Transportation Research Board, Washington, D.C., 2011.
17. Green, E.R., J.G. Pigman, J.R. Walton, and S. McCormack. Identification of Secondary Crashes and Recommended Countermeasures to Ensure More Accurate Documentation. Presented at 91st Annual Meeting of the Transportation Research Board, Washington, D.C., 2012.
18. Sun, C., and V. Chilukuri. Use of Dynamic Incident Progression Curve for Classifying Secondary Accidents. Presented at 85th Annual Meeting of the Transportation Research Board, Washington, D.C., 2006.
19. Chou, C.-S., and E. Miller-Hooks. Simulation-Based Secondary Incident Filtering Method. *Journal of Transportation Engineering,* Vol. 136, No. 8, 2010, pp. 746–754.
20. Zhang, H., and A. Khattak. What Is the Role of Multiple Secondary Incidents in Traffic Operations? *Journal of Transportation Engineering,* Vol. 136, No. 11, 2010, pp. 986–997.
21. Khattak, A.J., X. Wang, and H. Zhang. Spatial Analysis and Modeling of Traffic Incidents for Proactive Incident Management and Strategic Planning. In *Transportation Research Record: Journal of the Transportation Research Board, No. 2178,* Transportation Research Board of the National Academies, Washington, D.C., 2010, pp. 128–137.
22. Zhang, H., and A.J. Khattak. Analysis of Cascading Incident Event Durations on Urban Freeways. In *Transportation Research Record: Journal of the Transportation Research Board, No. 2178,* Transportation Research Board of the National Academies, Washington, D.C., 2010, pp. 30–39.
23. Orfanou, F.P., E.I. Vlahogianni, and M.G. Karlaftis. Detecting Secondary Accidents in Freeways. Presented at 3rd International Conference of Road Safety and Simulation, Washington, D.C., 2011.
24. Zhang, H., and A. Khattak. Spatiotemporal Patterns of Primary and Secondary Incidents on Urban Freeways. In *Transportation Research Record: Journal of the Transportation Research Board, No. 2229,* Transportation Research Board of the National Academies, Washington, D.C., 2011, pp. 19–27.
25. Vlahogianni, E.I., M.G. Karlaftis, and F.P. Orfanou. Modeling the Effects of Weather and Traffic on the Risk of Secondary Incidents. *Journal of Intelligent Transportation Systems,* Vol. 16, No. 3, 2012, pp. 109–117.
26. Yang, H., B. Bartin, and K. Ozbay. Use of Sensor Data to Identify Secondary Crashes on Freeways. In *Transportation Research Record: Journal of the Transportation Research Board, No. 2396,* Transportation Research Board of the National Academies, Washington, D.C., 2013, pp. 82–92.
27. Yang, H., B. Bartin, and K. Ozbay. Investigating the Characteristics of Secondary Crashes on Freeways. Presented at 92nd Annual Meeting of the Transportation Research Board, Washington, D.C., 2013.
28. Imprialou, M.M., F.P. Orfanou, E.I. Vlahogianni, and M.G. Karlaftis. Defining Spatiotemporal Influence Areas in Freeways for Secondary Accident Detection. Presented at 92nd Annual Meeting of the Transportation Research Board, Washington, D.C., 2013.
29. Chung, Y. Identifying Primary and Secondary Crashes from Spatiotemporal Crash Impact Analysis. In *Transportation Research Record: Journal of the Transportation Research Board, No. 2386,* Transportation Research Board of the National Academies, Washington, D.C., 2013, pp. 62–71.
30. Parker, S.T., and Y. Tao. WisTransPortal: A Wisconsin Traffic Operations Data Hub. Presented at 9th International Conference on Applications of Advanced Technology in Transportation, Chicago, Ill., 2006.
31. Parker, S. WisTransPortal Developer Wiki. transportal.cee.wisc.edu/resources/wiki/. Accessed Jan. 7, 2013.
32. Official State Trunk Highway System Maps. Wisconsin Department of Transportation. www.dot.wisconsin.gov/travel/maps/sth.htm. Accessed Jan. 7, 2013.
33. Dijkstra, E.W. A Note on Two Problems in Connexion with Graphs. *Numerische Mathematik,* Vol. 1, 1959, pp. 269–271.
34. Hurdle, V.F., and B. Son. Shock Wave and Cumulative Arrival and Departure Models: Partners Without Conflict. In *Transportation Research Record: Journal of the Transportation Research Board, No. 1776,* TRB, National Research Council, Washington, D.C., 2001, pp. 159–166.
35. Li, H., and R.L. Bertini. Comparison of Algorithms for Systematic Tracking of Patterns of Traffic Congestion on Freeways in Portland, Oregon. In *Transportation Research Record: Journal of the Transportation Research Board, No. 2178,* Transportation Research Board of the National Academies, Washington, D.C., 2010, pp. 101–110.
36. Saddi, R.R. Studying the Impacts of Primary Incidents on Freeways to Identify Secondary Incidents. MS thesis. University of Nevada, Las Vegas, 2009.

The Safety Data, Analysis, and Evaluation Committee peer-reviewed this paper.